

Electronic Supplementary Information (ESI)

Single-crystal-to-single-crystal transformation of a two-dimensional coordination polymer through highly selective [2+2] photodimerization of a conjugated dialkene

*Dong Liu, Hui-Fang Wang, Brendan F. Abrahams and Jian-Ping Lang**

*E-mail: jplang@suda.edu.cn

Table of Contents

General procedures.	S3
Preparation of $[\text{Zn}_4(\text{OH})_2(5\text{-NO}_2\text{-1,3-BDC})_2(5\text{-NO}_2\text{-1,3-HBDC})_2(\text{ppene})_2]_n$ (1)	S3
Preparation of $[\text{Zn}_4(\text{OH})_2(5\text{-NO}_2\text{-1,3-BDC})_2(5\text{-NO}_2\text{-1,3-HBDC})_2(\text{bpbpvc})_2]_n$ (2)	S3
X-ray diffraction crystallography	S4
Computational studies	S5
Table S1 Selected bond length (Å) and angle (°) of 1 and 2	S6
Fig. S1 The TGA curves for 1 and 2	S8
Fig. S2 Experimental (red) and simulated (black) PXRD patterns for 1 (a) and 2 (b).	S9
A detailed analysis of the PXRD data	S10
Structure Descriptions (Includes detailed structural descriptions and Fig. S3-S4).	S11
Fig. S5 The ^1H NMR spectra of 1 (a) and 2 (b) in $\text{DMSO-}d_6$ at ambient temperature.	S15
Fig. S6 Structural models of four possible photoproducts of ppene.	S16

General procedures. The ligand 4-pyr-poly-2-ene (ppene) was prepared as reported previously.¹ Other chemicals and reagents were purchased from TCI Co., Ltd., and Sigma-Aldrich Co. Powder XRD patterns were obtained using a PANalytical X'Pert PRO MPD system (PW3040/60). Thermal analysis was performed with a Perkin_Elmer TGA-7 thermogravimetric analyzer at a heating rate of 10 °C/min and a flow rate of 100 cm³/min (N₂). ¹H NMR spectra were recorded at ambient temperature on a Bruker ADVANCE III (400MHz) spectrometer. ¹H NMR chemical shifts were referenced to the solvent signal in *d*₆-DMSO. Infrared (IR) samples were prepared as KBr pellets, and spectrum was obtained in the 4000–400 cm⁻¹ range using a Nicolet Avatar 360 FT-IR spectrophotometer. The elemental analyses for C, H and N were performed on an EA1110 CHNS elemental analyzer.

1 X. Gao, T. Friščić, L. R. MacGillivray, *Angew. Chem., Int. Ed.* **2004**, *43*, 232.

Preparation of [Zn₄(OH)₂(5-NO₂-1,3-BDC)₂(5-NO₂-1,3-HBDC)₂(ppene)₂]_n (1): To a 50 mL Teflon-lined autoclave was loaded Zn(NO₃)₂·6H₂O (0.298g, 1 mmol), 5-NO₂-1,3-H₂BDC (0.211g, 1 mmol), ppene (0.209g, 1 mmol) and H₂O (25 mL). The Teflon-lined autoclave was sealed and heated in an oven to 170°C for 50 h, and then cooled to ambient temperature at a rate of 5°C h⁻¹ to form yellow blocks of **1**, which were washed with ethanol and dried in air. Yield: 0.337g (87% yield based on Zn). Anal. calcd. for C₃₀H₂₀N₄O₁₃Zn₂: C, 46.47; H, 2.60; N, 7.23. Found: C, 46.72; H, 3.01; N, 6.98. IR (KBr, cm⁻¹): 3425m, 3094w, 1716m, 1637s, 1560s, 1541s, 1508m, 1458m, 1385s, 1273m, 1221m, 1074m, 1021w, 987s, 924m, 869m, 842s, 797m, 729s, 648m, 572s, 436w. ¹H NMR (400 MHz, *d*₆-DMSO): δ = 8.78 (d, 8H, Py-H, ppene), 8.69 (s, 8H, Ph-H, 5-NO₂-1,3-BDC/5-NO₂-1,3-HBDC), 8.65 (s, 4H, Ph-H, 5-NO₂-1,3-BDC/5-NO₂-1,3-HBDC), 8.20 (d, 8H, Py-H, ppene), 7.82 (d, 4H, CH=CH, ppene), 7.25 (d, 4H, CH=CH, ppene).

Preparation of [Zn₄(OH)₂(5-NO₂-1,3-BDC)₂(5-NO₂-1,3-HBDC)₂(bpbpvcb)]_n (2): Single

crystals of **1** (0.233 g) were irradiated by Hg lamp (400 W) for about 60 h to form crystals of **2** in a quantitative yield (based on **1**). Anal. calcd. for $C_{30}H_{20}N_4O_{13}Zn_2$: C, 46.47; H, 2.60; N, 7.23. Found: C, 46.66; H, 2.73; N, 7.01. IR (KBr, cm^{-1}): 3424m, 3094w, 1712m, 1631s, 1532s, 1507m, 1454m, 1426m, 1343s, 1278m, 1226m, 1186m, 1094w, 1075m, 986s, 926m, 869m, 843s, 784m, 728s, 647m, 570s, 426w. 1H NMR (400 MHz, d_6 -DMSO): δ = 8.76 (d, 8H, Py-H, bpbpvcb), 8.68 (s, 8H, Ph-H, 5-NO₂-1,3-BDC/5-NO₂-1,3-HBDC), 8.65 (s, 4H, Ph-H, 5-NO₂-1,3-BDC/5-NO₂-1,3-HBDC), 8.18 (d, 4H, Py-H, bpbpvcb), 7.93 (d, 4H, Py-H, bpbpvcb), 7.02 (d, 2H, CH=CH, bpbpvcb), 6.83 (d, 2H, CH=CH, bpbpvcb), 4.61 (d, 4H, CH-CH, bpbpvcb).

X-ray diffraction crystallography. All measurements were made on a Rigaku Mercury CCD X-ray diffractometer by using graphite monochromated Mo $K\alpha$ ($\lambda = 0.071073$ nm). Single crystals of **1** and **2** suitable for X-ray analysis were mounted on glass fibers and cooled at 223 K in a liquid nitrogen stream. Cell parameters were refined on all observed reflections by using the program *Crystalclear* (Rigaku and MSc, Ver. 1.3, 2001). The collected data were reduced by the program *CrystalClear*, and an absorption correction (multiscan) was applied. The reflection data were also corrected for Lorentz and polarization effects. The structures were solved by direct methods, and nonhydrogen atoms were refined anisotropically by least-squares on F^2 using the *SHELXTL-97* program.² The H atom of 5-NO₂-1,3-HBDC ligand and -OH group in **1** and **2** were located from the Fourier map. All other H atoms were introduced at the calculated positions and included in the structure-factor calculations.

2 (a) G. M. Sheldrick, *SHELXS-97, Program for the refinement of crystal structures*, University of Göttingen, Germany. 1997; (b) G. M. Sheldrick, *SHELXL-97, Program for Refinement of Crystal Structures*, University of Göttingen, Germany. 1997.

Crystal data for 1: $C_{30}H_{20}N_4O_{13}Zn_2$, $M_r = 775.28$, triclinic, space group $P\bar{1}$, $a = 10.905(2)$, $b = 12.399(3)$, $c = 11.809(2)$ Å, $\alpha = 79.53(3)$, $\beta = 74.15(3)$, $\gamma = 89.19(3)^\circ$, $V = 1509.4(6)$ Å³, $Z = 2$,

$\rho_{\text{calcd}} = 1.706 \text{ g/cm}^3$, $\mu(\text{Mo K}\alpha) = 1.667 \text{ cm}^{-1}$, $R_1 = 0.0330$ ($I > 2\sigma$), $wR_2 = 0.1036$, $GOF = 1.045$.

Crystal data for 2: $\text{C}_{30}\text{H}_{20}\text{N}_4\text{O}_{13}\text{Zn}_2$, $M_r = 775.28$, triclinic, space group $P\bar{1}$, $a = 11.092(2)$, $b = 11.997(2)$, $c = 12.063(2) \text{ \AA}$, $\alpha = 78.43(3)$, $\beta = 73.91(3)$, $\gamma = 89.64(3)^\circ$, $V = 1508.9(5) \text{ \AA}^3$, $Z = 2$, $\rho_{\text{calcd}} = 1.706 \text{ g/cm}^3$, $\mu(\text{Mo K}\alpha) = 1.667 \text{ cm}^{-1}$, $R_1 = 0.0715$ ($I > 2\sigma$), $wR_2 = 0.1537$, $GOF = 1.117$.

Computational studies. All calculations were performed using Gaussian 09.³ The geometry optimizations were optimized using B3LYP functional⁴ with the triple zeta basis set 6-311++G(d,p).⁵ No symmetry constraints were imposed. Analytical frequencies were calculated to verify the nature of all stationary points as minima.

3 M. J. Frisch, G. W. Trucks, H. B. Schlegel, G. E. Scuseria, M. A. Robb, J. R. Cheeseman, G. Scalmani, V. Barone, B. Mennucci, G. A. Petersson, H. Nakatsuji, M. Caricato, X. Li, H. P. Hratchian, A. F. Izmaylov, J. Bloino, G. Zheng, J. L. Sonnenberg, M. Hada, M. Ehara, K. Toyota, R. Fukuda, J. Hasegawa, M. Ishida, T. Nakajima, Y. Honda, O. Kitao, H. Nakai, T. Vreven, J. A. Montgomery, Jr., J. E. Peralta, F. Ogliaro, M. Bearpark, J. J. Heyd, E. Brothers, K. N. Kudin, V. N. Staroverov, T. Keith, R. Kobayashi, J. Normand, K. Raghavachari, A. Rendell, J. C. Burant, S. S. Iyengar, J. Tomasi, M. Cossi, N. Rega, J. M. Millam, M. Klene, J. E. Knox, J. B. Cross, V. Bakken, C. Adamo, J. Jaramillo, R. Gomperts, R. E. Stratmann, O. Yazyev, A. J. Austin, R. Cammi, C. Pomelli, J. W. Ochterski, R. L. Martin, K. Morokuma, V. G. Zakrzewski, G. A. Voth, P. Salvador, J. J. Dannenberg, S. Dapprich, A. D. Daniels, O. Farkas, J. B. Foresman, J. V. Ortiz, J. Cioslowski and D. J. Fox, Gaussian 09, Revision C.01, Gaussian, Inc., Wallingford CT, 2010.

4 (a) A. D. Becke, *J. Chem. Phys.*, 1993, **98**, 5648; (b) C. Lee, W. Yang and R. G. Parr, *Phys. Rev. B.*, 1988, **37**, 785.

5 M. P. Andersson and P. J. Uvdal, *Phys. Chem. A*, 2005, **109**, 2937.

Table S1. Selected Bond Lengths (Å) and Angles (°) for 1 and 2.

Compound 1			
Zn(1)-O(13)	1.942(2)	Zn(1)-O(1)	1.957(2)
Zn(1)-O(7)	1.967(2)	Zn(1)-N(1A)	2.001(3)
Zn(2)-O(12B)	2.064(2)	Zn(2)-O(8)	2.096(2)
Zn(2)-O(13C)	2.096(2)	Zn(2)-N(2)	2.114(2)
Zn(2)-O(13)	2.1233(19)	Zn(2)-O(2)	2.155(2)
O(13)-Zn(1)-O(1)	99.69(9)	O(13)-Zn(1)-O(7)	114.92(9)
O(1)-Zn(1)-O(7)	120.87(10)	O(13)-Zn(1)-N(1A)	116.43(10)
O(1)-Zn(1)-N(1A)	104.08(10)	O(7)-Zn(1)-N(1A)	101.23(10)
O(12B)-Zn(2)-O(8)	172.59(9)	O(12B)-Zn(2)-O(13C)	93.78(8)
O(8)-Zn(2)-O(13C)	90.05(9)	O(12B)-Zn(2)-N(2)	86.27(9)
O(8)-Zn(2)-N(2)	87.00(9)	O(13C)-Zn(2)-N(2)	96.51(9)
O(12B)-Zn(2)-O(13)	95.18(8)	O(8)-Zn(2)-O(13)	91.72(8)
O(13C)-Zn(2)-O(13)	80.35(8)	N(2)-Zn(2)-O(13)	176.61(8)
O(12B)-Zn(2)-O(2)	86.10(9)	O(8)-Zn(2)-O(2)	91.18(9)
O(13C)-Zn(2)-O(2)	170.43(7)	N(2)-Zn(2)-O(2)	93.04(9)
O(13)-Zn(2)-O(2)	90.12(8)		
Compound 2			
Zn(1)-O(11A)	2.075(4)	Zn(1)-O(8)	2.088(4)
Zn(1)-N(2B)	2.102(5)	Zn(1)-O(13)	2.105(4)
Zn(1)-O(13C)	2.153(5)	Zn(1)-O(1)	2.160(5)

Zn(2)-O(13)	1.972(4)	Zn(2)-O(7)	1.979(4)
Zn(2)-O(2)	1.987(5)	Zn(2)-N(1)	2.055(5)
O(11A)-Zn(1)-O(8)	174.99(18)	O(11A)-Zn(1)-N(2B)	86.08(18)
O(8)-Zn(1)-N(2B)	89.10(18)	O(11A)-Zn(1)-O(13)	94.64(18)
O(8)-Zn(1)-O(13)	90.25(18)	N(2B)-Zn(1)-O(13)	176.34(19)
O(11A)-Zn(1)-O(13C)	89.57(18)	O(8)-Zn(1)-O(13C)	91.96(18)
N(2B)-Zn(1)-O(13C)	92.10(19)	O(13)-Zn(1)-O(13C)	84.32(16)
O(11A)-Zn(1)-O(1)	88.60(18)	O(8)-Zn(1)-O(1)	90.31(19)
N(2B)-Zn(1)-O(1)	93.05(19)	O(13)-Zn(1)-O(1)	90.56(17)
O(13C)-Zn(1)-O(1)	174.41(17)	O(13)-Zn(2)-O(7)	111.94(18)
O(13)-Zn(2)-O(2)	99.16(18)	O(7)-Zn(2)-O(2)	121.7(2)
O(13)-Zn(2)-N(1)	122.8(2)	O(7)-Zn(2)-N(1)	101.8(2)
O(2)-Zn(2)-N(1)	100.4(2)		

Symmetry codes: **(1)** A: $x, y + 1, z + 1$; B: $x - 1, y, z$; C: $-x + 1, -y + 2, -z + 1$. **(2)** A: $x + 1, y, z$;

B: $x, y + 1, z + 1$; C: $-x + 1, -y + 1, -z + 2$.

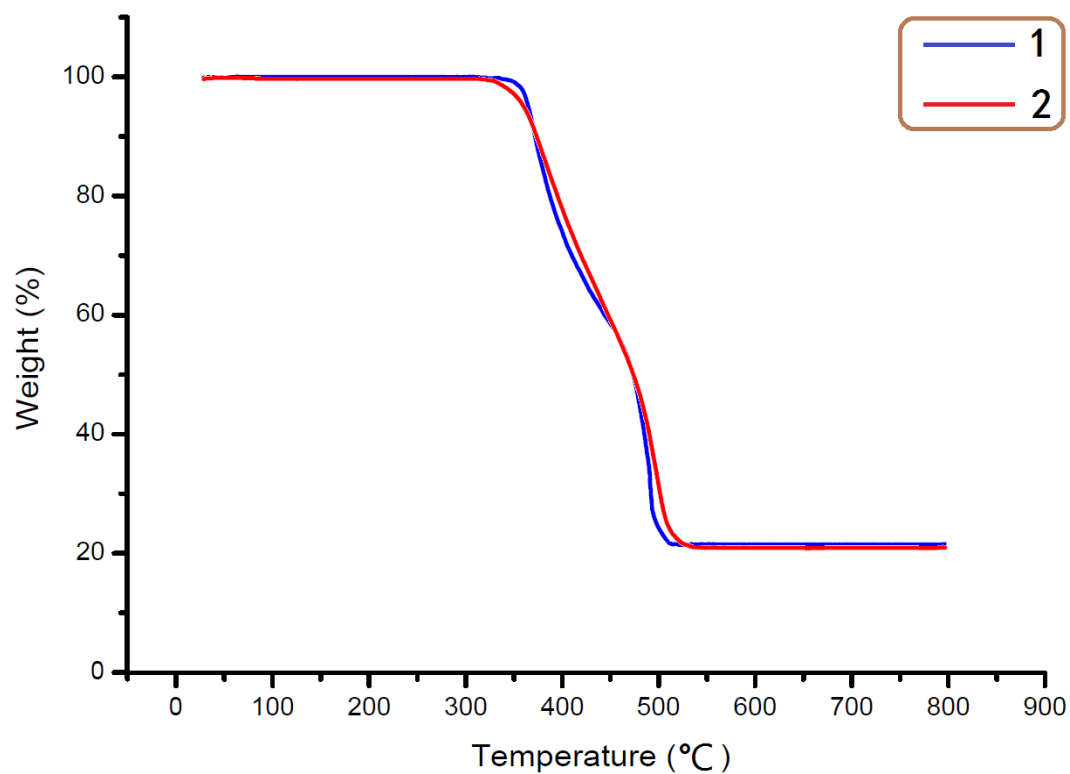


Fig. S1 The TGA curves for **1** and **2**. Compound **1** is stable up to about 340°C upon at which temperature decomposition is observed. The TGA curve of **2** is similar to that of **1**. The final residues were assumed to be ZnO (ca. 20.99%), which is consistent with the experimental weights of residues (21.35% for **1** and 20.53% for **2**).

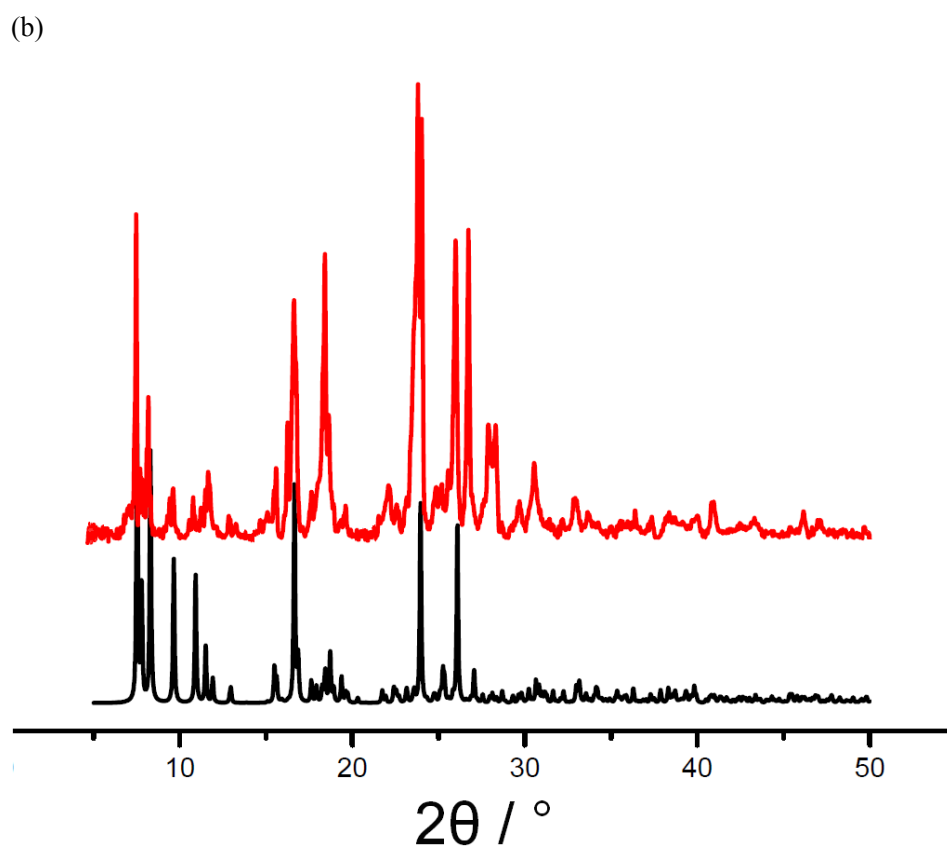
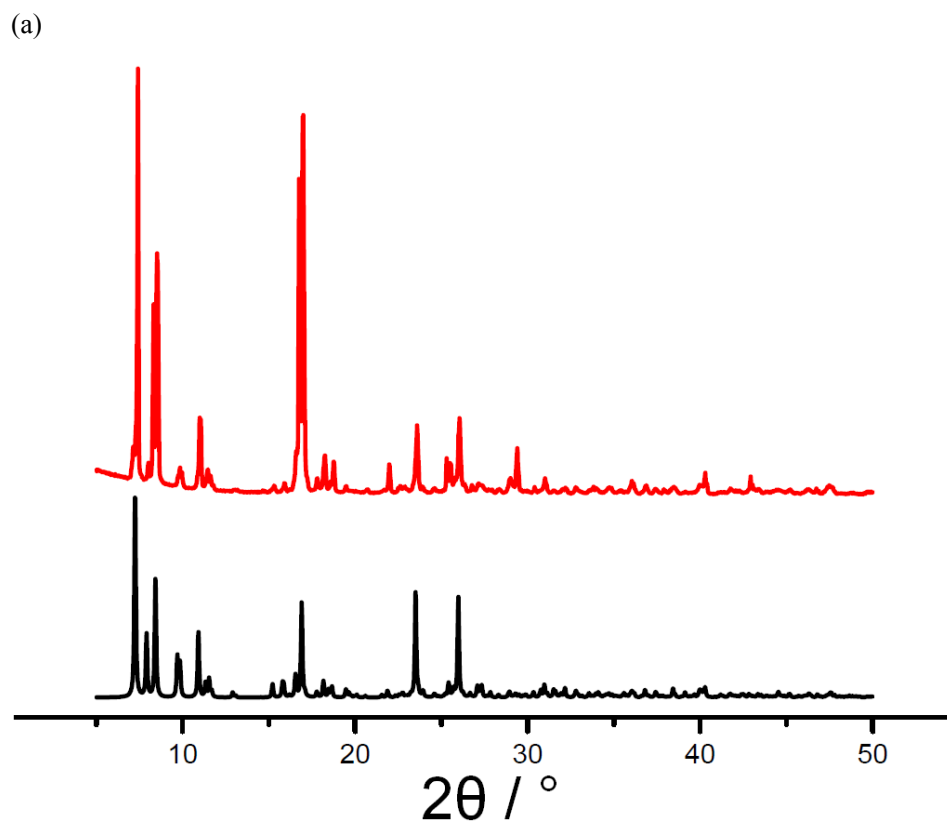


Fig. S2 Experimental (red) and simulated (black) PXRD patterns for **1** (a) and **2** (b).

A detailed analysis of the PXRD data

For each compound, the detailed data for the seven strongest peaks were listed as follows. The FWHM values of these peaks exhibit more or less differences between **1** and **2**, which indicated that **1** and **2** are two different complexes.

Compound 1:

Beginning / °	Ending / °	Center / °	FWHM / °
7.1844	7.696	7.5779	0.06751
8.3258	8.8571	8.68	0.17152
10.9824	11.317	11.1595	0.14459
16.5516	17.4568	17.1616	0.13805
23.4983	23.9115	23.7541	0.15798
25.8204	26.4108	26.214	0.1555
29.4413	29.6775	29.5594	0.12527

Compound 2:

Beginning / °	Ending / °	Center / °	FWHM / °
6.7418	7.5683	7.4699	0.08811
7.5683	8.3555	8.1784	0.15557
16.3452	16.9355	16.6207	0.30598
17.7424	18.5492	18.4114	0.21079
23.0163	23.9412	23.8035	0.26661
25.4369	26.224	25.9879	0.20363
26.4798	26.9915	26.7357	0.14573

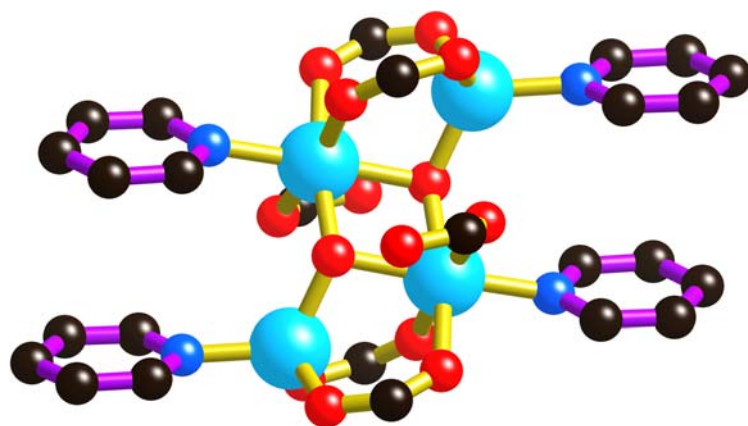
Structure Descriptions

Compound 1

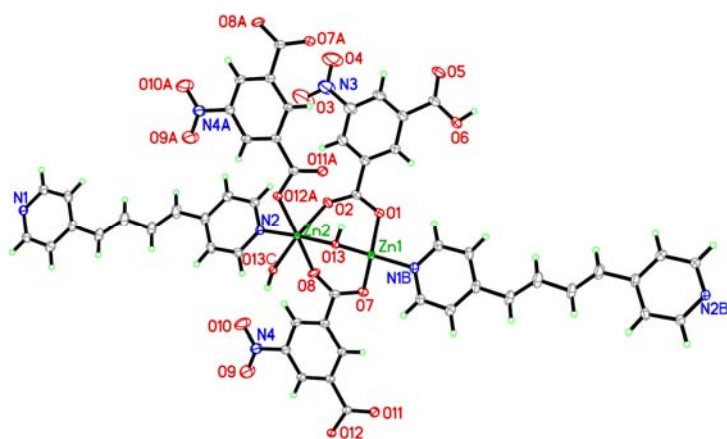
Within the structure of **1** a cluster of four Zn centers is coordinated by six carboxylate groups and a pair of μ_3 -hydroxide ions as shown in Fig. S3a. There are two types of crystallographically distinct Zn centers in the $Zn_4(OH)_2$ aggregate. The coordination modes of Zn1 and Zn2 are described as shown in Fig. S3b. In **1**, Zn1 is coordinated by five oxygen atoms and Zn2 is bound to three oxygen atoms. Four of the carboxylate groups belong to two pairs of bridging 5-NO₂-1,3-BDC ligands which link the $Zn_4(OH)_2$ aggregate into an infinite chain (Fig. S3c). Fig. S3c also shows carboxylate groups that are each part of a non-bridging ligand bound to the Zn centers. The non-coordinated carboxylate groups of these ligands are in fact protonated.

Octahedral and tetrahedral coordination geometries for each of the Zn(II) centers is attained through coordination of pyridyl groups from the ppene ligands. Each $Zn_4(OH)_2$ aggregate is bridged by two pairs of ppene ligands to equivalent $Zn_4(OH)_2$ aggregates belonging to neighboring parallel chains. Overall this gives rise to a 2D polymeric network that has the topology of a 4,4-net if the $Zn_4(OH)_2$ aggregate is considered as a node and pairs of ppene ligands and dicarboxylate ligands act as connections between the nodes (Fig. S3d). Neighboring sheets are linked by hydrogen bonds that extend from the non-coordinated carboxylic acid group to a non-coordinated carboxylate oxygen atom belonging to a bridging ligand of a parallel network.

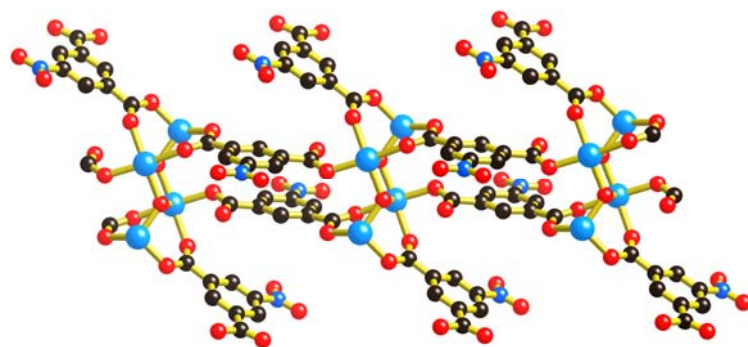
a)



b)



c)



d)

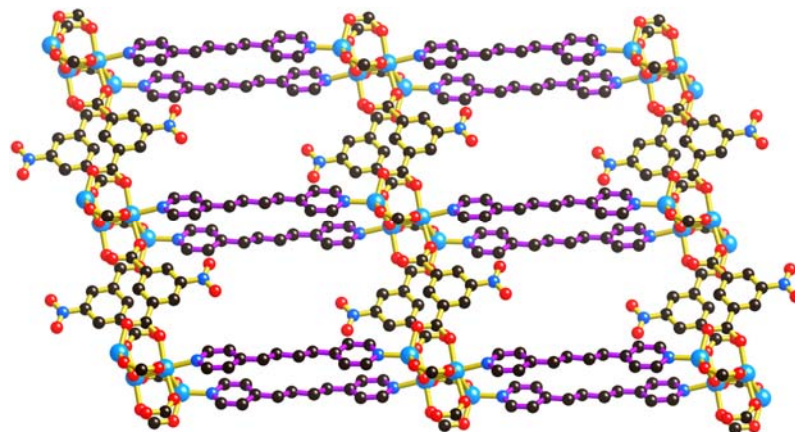
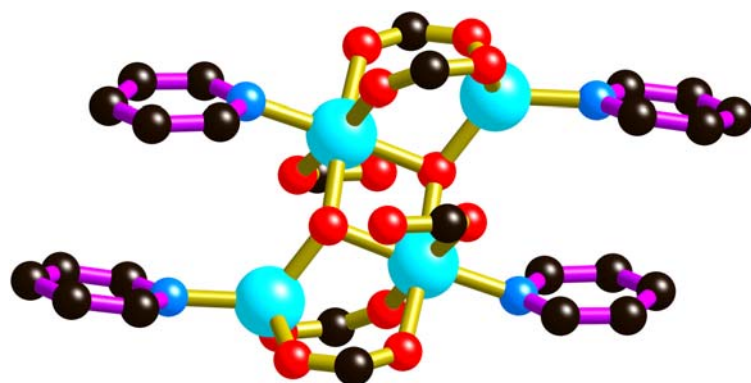


Fig. S3 The structure of compound **1**. a) View of the tetranuclear zinc aggregate in **1**. b) ORTEP drawing around Zn1 and Zn2 atoms in **1** at the 30% probability level. c) $Zn_4(OH)_2$ aggregates bridged by pairs of dicarboxylate within an infinite chain; pyridyl groups have been omitted. d) The 2D sheet formed by linking the $Zn_4(OH)_2$ -carboxylate chains with pairs of ppene ligands. Color code: C black, N blue, O red, Zn cyan. Hydrogen atoms have been omitted for clarity.

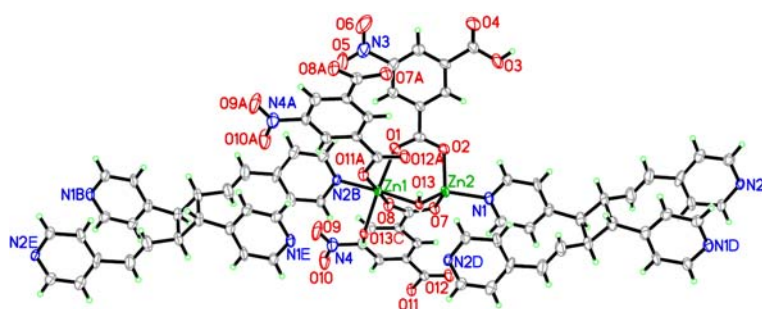
Compound 2

The structure of compound **2** closely resembles compound **1** except that the pair of closely associated ppene ligands have been replaced by a single tetrapyrridyl ligand (Fig. S4). The figures clearly indicate that relatively little rearrangement of the structure occurs upon dimerization of the ppene ligands. The transformation process involves the replacement of each pair of bidentate ppene ligands, that bridge $[Zn_4(OH)_2]$ nodes, with a single tetradentate ligand that links the same pair of nodes. Thus, from a topological perspective, the structure of **1** is preserved in the transformation, if the $[Zn_4(OH)_2]$ aggregates are considered as 4-connecting nodes. The cyclobutane unit within the new bpbpvcb molecule consists of four stereogenic centers, however with the cyclobutane ring centred on a centre of inversion, only the *meso* isomer is observed.

a)



b)



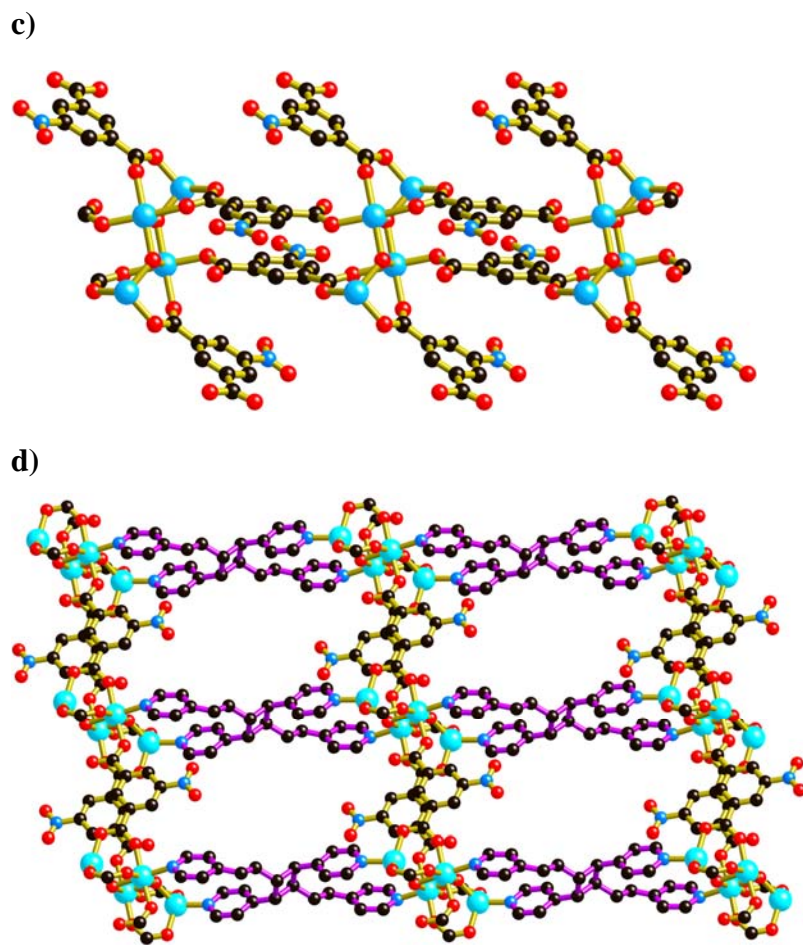
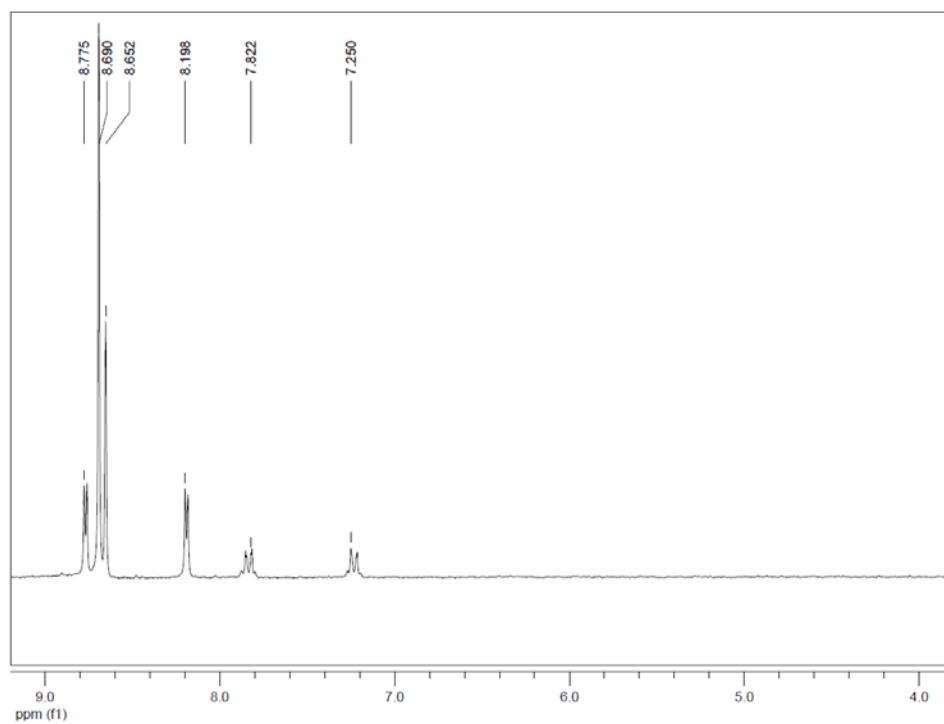


Fig. S4 The structure of compound **2**. a) View of the tetranuclear zinc aggregate in **2**. b) ORTEP drawing around Zn1 and Zn2 atoms in **2** at the 30% probability level. c) $Zn_4(OH)_2$ aggregates bridged by pairs of dicarboxylate within an infinite chain; pyridyl groups have been omitted. d) The 2D sheet formed by linking the $Zn_4(OH)_2$ -carboxylate chains with the tetrapyrrolyl ligand, bpbpvcb. Color code: C black, N blue, O red, Zn cyan. Hydrogen atoms have been coordinated for clarity.

(a)



(b)

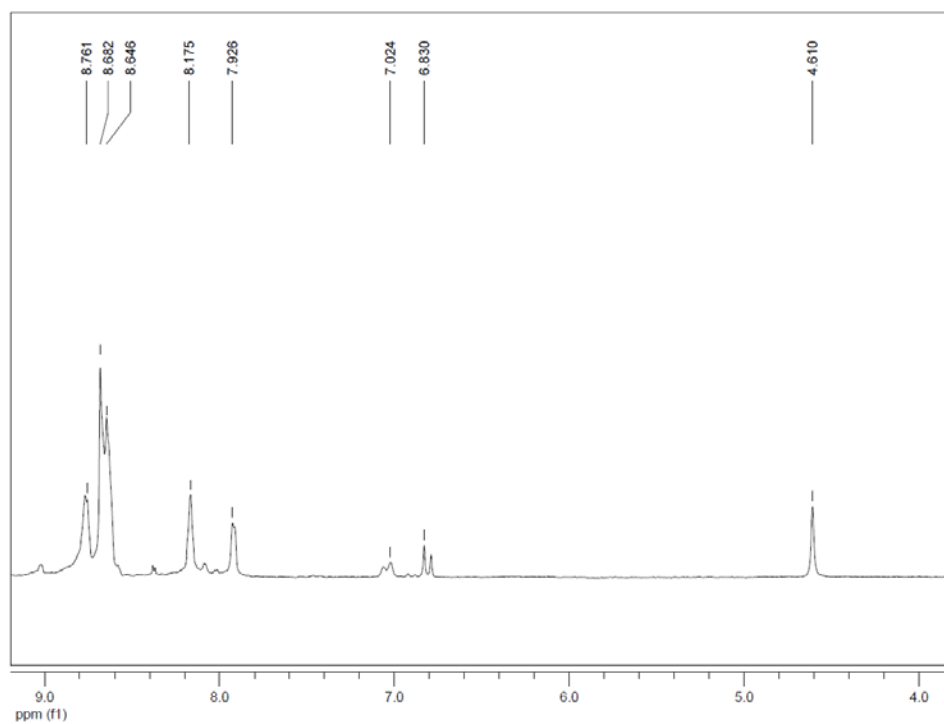


Fig. S5 The ¹H NMR spectra of **1** (a) and **2** (b) in DMSO-*d*₆ at ambient temperature.

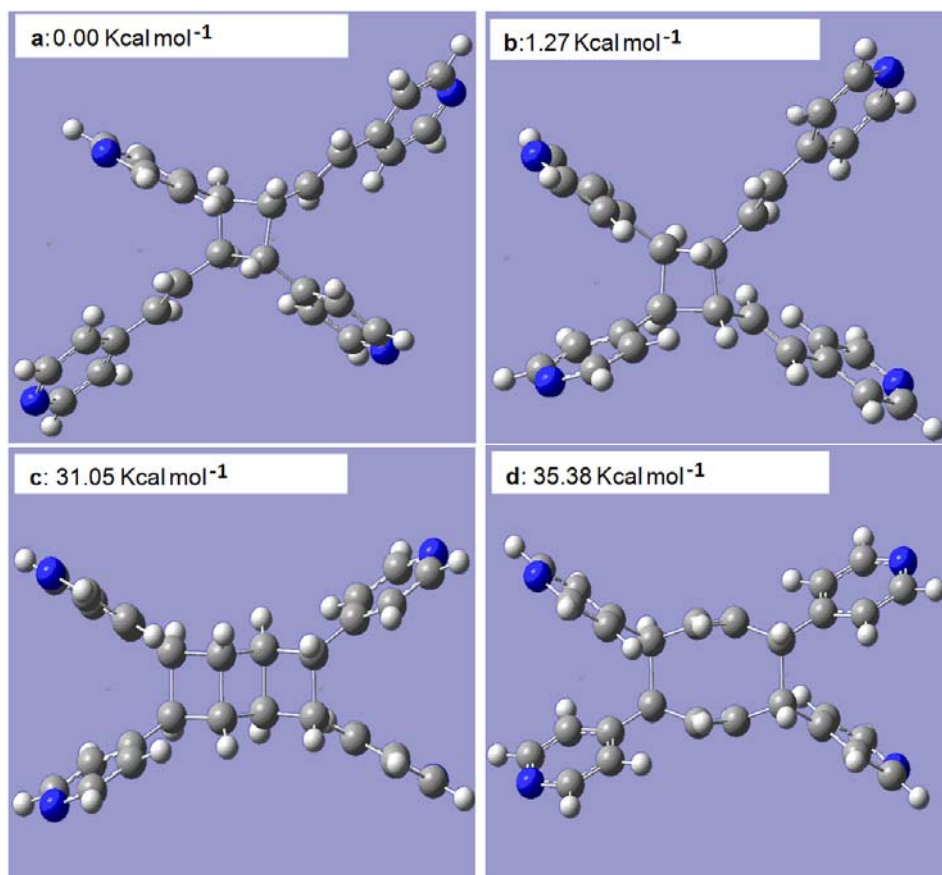


Fig. S6 Structural models of four possible photoproducts of ppene. The relative free energies (at 298.15K) compared to that of product **a** are listed in insets. For simplicity, the Zn atoms and other auxiliary fragments in the X-ray crystal structures were not taken into consideration.